Verification of Direct Walk

A Fast Pre-Selection Procedure Of Neutrino Candidates For The AMANDA and IceCube Detector

Abstract

After an introduction into neutrino astrophysics and the AMANDA experiment I compare the first-guess-methods *DirectWalk*, *LineFit* and *DipoleFit* in relation to their resolutions, fake-rates and efficiencies. *DirectWalk* is discussed in detail. I used the *IceRec*-software and standard F2K-AMASIM-dcorsica files (2003 detector configuration for AMANDA and 9string geometry for IceCube). The results are promising to use *DirectWalk* as the best first-guess-method for AMANDA and IceCube.

DESY Summer Student Programm 2006

Jan Dobschinski[1]

[1] Institute of Astrophysics Göttingen, D-37077,Göttingen, Germany

Contents

1 Introduction

2 The Neutrino

The neutrino is an elemantary particle with no charge and very little mass, that interacts only by the weak force and by gravity. It is a member of the lepton family of particles. Neutrinos travel at or close to the speed of light. Because of the small scattering cross-section they have only few interactions with matter, it has been calculated that neutrinos could pass through 100 light-years of solid lead with only a 50 percent chance of being absorbed.
The existence of neutrinos was first postulated in 1930 by Wolfgang Pauli [1] to ensure conservation of energy and angular momentum in beta decays. Three different types of neutrinos exist, known as electron-, mu-, and tau-neutrinos, corresponding to the massive leptons electron, muon, and tau.
The Sun produces neutrinos from thermonuclear fusion reactions in its core and, since these neutrinos pass cleanly through the Sun and all the way to Earth, they provide a glimpse into the heart of a star. Large fluxes of neutrinos carry away most of the energy of a supernova and neutrinos are one of the candidates for dark matter. So, neutrino astronomy offers an important new window on the universe beyond the electromagnetic spectrum. Because neutrinos pass so easily through matter, they are very hard to detect. Therefore you need a large volume in a transparent medium to use the effects of Cherenkov radiation.

3 Neutrino Astrophysics

Astrophysics with high energy neutrinos opens a new window for a better understanding of the universe [2]. The aim is to find answers to fundamental questions about the origin of cosmic rays, the search for candidates for cosmic accelerators by means of detecting point sources of high energy neutrinos and the search of dark matter and magnetic monopols.

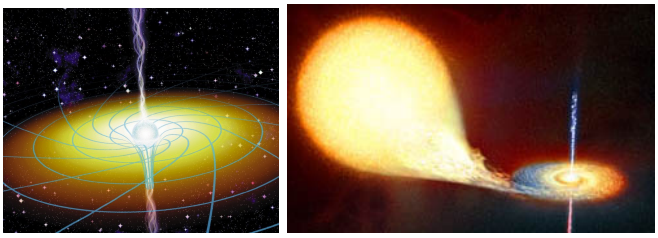

Figure 1: left: A black hole accretes matter from the torus so that relativistic jets of matter are ejected along the rotation axis. right: In a binary system in which a normal star (e.g. red giant) orbits around, and loses matter to, a nearby compact object, either a black hole or a neutron star (Microquasar)

3.1 Neutrino-sources and Acceleration

Sources of such high accelerations are for example *Active Galactic Nuclei*. The models about such galaxies assume that they have a central torus of dust and gas and a very massive black hole in the core. In case of the very strong gravitational forces, the black hole accretes matter from the torus, which flows inward the accretion disk. Due to the rotation of the black hole, magnetic field lines get bent at the poles so that highly relativistic jets of matter are ejected along the rotation axis (see figure 1).

An other possible source is a *Micro-Quasar*. In a binary system in which a normal star (e.g. red giant) orbits around, and loses matter to, a nearby compact object, either a black hole or a neutron star (see figure 1).

In case of a *supernova and shock fronts of supernova remnants* a lot of high energy neutrinos will also produced. More possible sources are *Pulsars, Gamma Ray Bursts, WIMP annihilation* and interactions of cosmic rays with interstellar matter or the microwave background radiation [3].

Electrons and protons are accelerated mostly by a process called *Fermi acceleration* in astronomical sources.[4] In an interstellar cloud, magnetic field lines are co-moving with the matter according the laws of magneto hydrodynamics. If a slow particle hits such a high velocity region, the thermodynamic equipartition of energy leads to acceleration of this particles. These is the first order Fermi acceleration. In contrast, when the acceleration takes place across a shock front, the energy gain is linear proportional on the shock velocity and you call this process second order Fermi acceleration.
These highly accelerated energetic particles interact with ambient particles or photon fields and produce secondary particles. Mesons are commonly produced if the flux of accelerated particles contains a hadronic component. High energy neutrinos are produced in the decay of these mesons. The decay of charged pions are of more interest here as they decay in high energy neutrinos:

$$\pi^+ \to \mu^+ + \nu_\mu \qquad \mu^+ \to e^+ + \nu_e + \overline{\nu_\mu}$$

$$\pi^- \to \mu^- + \overline{\nu_\mu} \qquad \mu^- \to e^- + \overline{\nu_e} + \nu_\mu$$

From pion decay we thus expected the neutrino flux to be produced at the source flavor ratio

$$F(\nu_e) : F(\nu_\mu) : F(\nu_\tau) = 1 : 2 : 0$$

Propagating their way the neutrinos undergo oscillations and have the following flavor ratio at earth:

$$F(\nu_e) : F(\nu_\mu) : F(\nu_\tau) = 1 : 1 : 1$$

3.2 Neutrino Reactions and Detection

The main method to detect high-energy neutrinos are scattering processes (only reactions of high energetic particles are discussed here).

Neutrinos can not interact electromagnetically, but through the weak interaction by the exchange of $W^{\pm}$- or Z^0-bosons. The major interactions are charged and neutral current reactions:

$$\nu_l + N \rightarrow l + X(CC)$$

$$\nu_l + N \rightarrow \nu_l + X(NC)$$

where l represents any lepton e,μ or τ and the nucleon N is transferred into another hadronic state X. The cross sections for these reactions are very small. For neutrino telescopes one distinguishes between the muon channel (based on $\nu_\mu + N \rightarrow \mu + X$), and the cascade channel (based on all other reactions). In this report I only investigated on the muon channel.

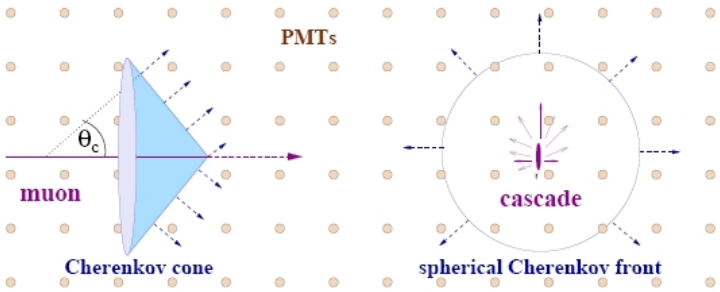

Figure 2: Detection modes of the AMANDA detector. left: muon channel, right: the cascade channel of electron- and tau-neutrinos [5]

If a high energy neutrino creates a muon, this muon is nearly collinear with the neutrino direction (deviation angle $\psi = 0.7° x (E_\nu / TeV)^{-0.7}$). Therefore you need, to identify the direction of the neutrinos a accurate requirement for reconstruction of $\leq 1°$ [5] [6]. If this high energy muon flies through the ice or water, it emits Cherenkov light in a cone. The angle of the cone can be calculated: $cos\Theta = (n\beta)^{-1}$ with n as the index of refraction in the medium. In case of relativistic particles and ice $\beta \cong 1$ and $n \cong 1.32$ and you get $\Theta \approx 41°$. You have also radiative energy loss processes which generate secondary charged particles which also emits Cherenkov light which you can use for calculate roughly the muon energy.
These Cherenkov signals can be observed with photo-multipliers. The both detection modes of the muon and the cascade channel are sketched in figure 2.

4 The Antarctic Muon and Neutrino Detector Array (AMANDA)

4.1 General Remarks

AMANDA is a neutrino detector at the geographic south pole [4][7][8][9]. Because of the long free track-length of muons AMANDA has a large volume of about $0.03km^3$. The detector consists of 677 photo-multiplier-tubes which are fixed on 19 strings in form of a lattice (see figure 3). These optical modules

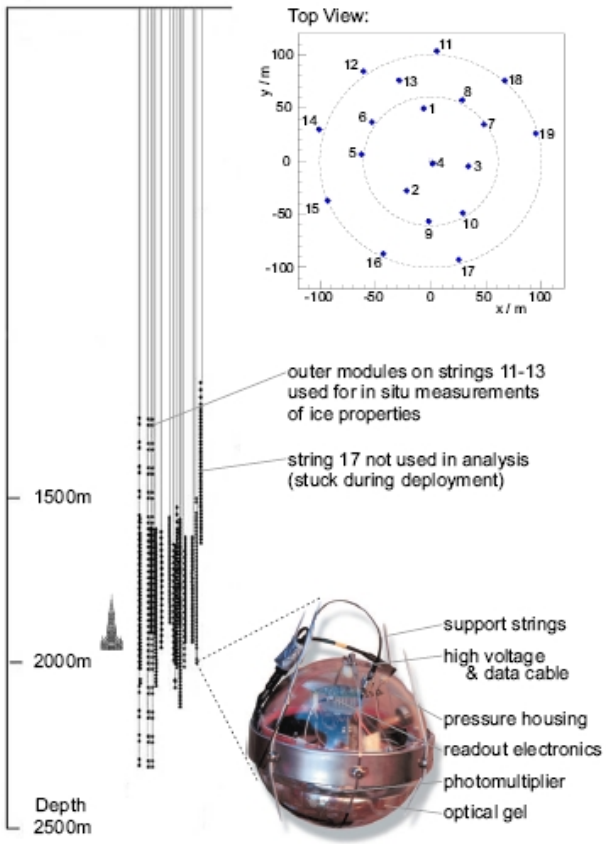

Figure 3: A sketch of the AMANDA II geometry. Top right you see a view on the top of the detector. On Left the location of the several strings is shown to compare the size of the detector with the Münster of Ulm and bottom left you see a picture with description of an optical module. [4]

(OM) are melted into the ice using hot water. After some days the holes refreezes and the strings and modules are fixed. The depth of the strings reached

from about 1250m up to 2300m.This position was chosen after some tests in 1993/94 with AMANDA-A.AMANDA-A consisted of 4 strings which had only a depth up to one kilometer. This depth wasn't suitable because air bubbles lead to scattering lengths of only $\approx 25cm$. In bigger depth, with increasing pressure, these air bubbles are compressed and a suitable position reached.In 1999/2000 the detector reached his present state and was labelled AMANDA II. In figure 3 you can see in which form and distances the strings and OMs are located.
The primary goal of this detector is to detect high-energy neutrinos from astrophysical sources and determine their arrival time, direction and energy.

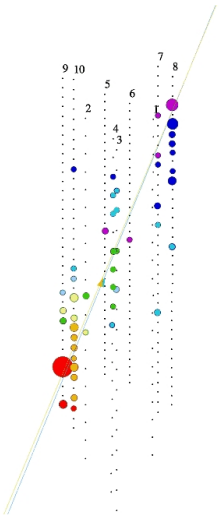

Figure 4: The points are photo-multipliers, and the colors represent the arrival time: from red (early hits) via green, yellow, blue to violette (latest hits). The size of the points are proportional to the amplitude.

4.2 Optical Moduls

The OMs are sphere vessels with photo-multiplier inside in pressure housing. In the upper half of the OM the high voltage support and the readout electronics are located (see figure 3). In the lower half there are the photo-multipliers themselves and optical contact gel. The AMANDA modules are analog devices, the signals will be digitalized at the surface by an analog-to-digital-converter which records the peak values and a time-to-digital-converter which records the start and end time for each pulse (see figure 4).
A full event is registered if a trigger condition is fulfilled. Important to know is that an event is written if 24 OMs are hit within a time-window of $2.5\mu s$. The trigger rate is around 80Hz and varies with different detector setups and atmospheric densities.

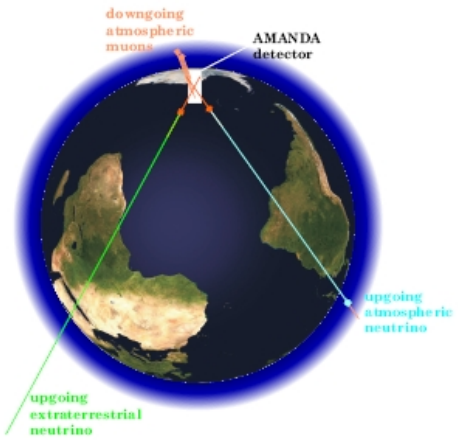

Figure 5: Here you see the several event classes which are observed with AMANDA. On the one site there are the down-going atmospheric muons and on the other site the up-going atmospheric neutrinos and the up-going extraterrestrial neutrinos which penetrated the complete earth before they are detected. For the AMANDA experiment the up-going extraterrestrial neutrinos are the most important.[4]

4.3 Signal and Background

The most abundant events in AMANDA are atmospheric muons. These muons are created by cosmic rays interacting with the earth atmosphere and are called *down-going-muons* (see figure 5). They form the background in the search for atmospheric and extra-terrestrial neutrinos.

The number of this muons is five orders of magnitude bigger then the muons from atmospheric neutrinos. The signal neutrinos are the up-going extraterrestrial neutrinos which creates muons by scattering with nucleons in the earth. Only these neutrinos are used to find distant astrophysical sources.

4.4 IceCube

IceCube will be the biggest particle detector world-wide with a volume of about one cubic kilometer and 4800 optical modules (see figure 6)[2]. The work will be completed in 2011. The IceCube (and AMANDA) optical sensors are so sensitive that they will respond even on a single photon. Unlike AMANDA, the signals in IceCube optical modules will be amplified, converted into electrical pulses and then translated into digital signals with onboard mini-computers.

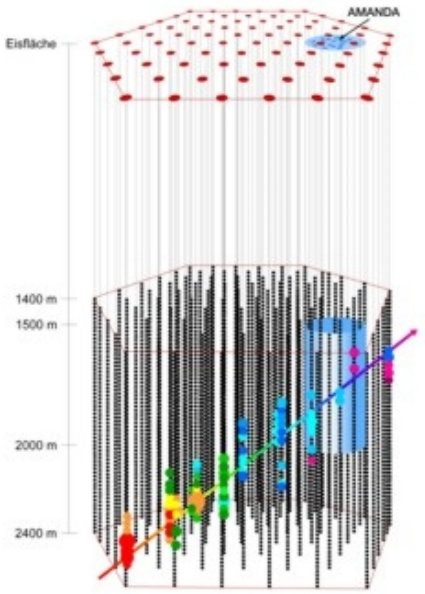

Figure 6: A sketch of the IceCube-detector to compare size with AMANDA (top rigth).[2]

5 Reconstruction procedures for fast pre-selection of neutrino candidates

5.1 General Remarks

It is necessary to have well working fast pre-selection method, because of limited bandwidth to write data over satelltite to the North. The pre-selection method decides that an event is useful for a further analysis with the reconstruction procedure (*Likelihood methods*). If the pre-selection method can not reconstruct or badly reconstruct an event, it will be deleted completely. AMANDA using currently *DirectWalk* as on-line filtering on the pole, whereas IceCube uses *LineFit* and *DipoleFit*. Therefore it is the good of my work to decide if *DirectWalk* could also work with the present IceCube geometry.

5.2 DirectWalk

DirectWalk (DW) is a very efficient first guess method with a pattern recognition algorithm and is optimized for background suppression. It is important to know

that DW do not need any external hit-cleaning. DW works in four steps:

1. *TREL-selection*: The procedure is searching for track elements. A TREL is a coincidence of two direct hits and all 2-hit combinations are selected and analyzed with the following time- and distance-requirement:

$$D/c - 30ns < \Delta t < D/c + 30ns$$

   with D>50m. Δt is the time difference between two hits.

2. *CAND-selection*: To be a track candidate (CAND) the TREL-parameters must describe the typical pattern of a muon track which are a sufficient number of hits along the track and a minimum track length. The quality criteria are in the $\delta t - \rho - plane$ are:

$$-50ns < \delta t < 300ns$$

$$\rho < 25x\sqrt[4]{\delta t + 50ns}$$

   You need also a quality criteria to guaranty a minimum track quality:

$$N_{hit} > 10$$

$$\sigma_L = \frac{1}{N}\Sigma(L_i - \overline{L})^2 \geq 20m$$

   σ_L is the spread along the track.

3. *TRACK-selection*: In this step the best track candidate will be searched with a cluster-in-space method.

4. *TRACK-direction*: In the last step the procedure calculate the track direction of the best track candidate and the fitting parameters are stored. A detailed description is given by P.Steffen [10] [11].

5.3 LineFit

LineFit(LF) is a very simple, robust method like a linear regression. Cherenkov cones and properties of the medium are completely ignored. LF calculates an initial track on the basis of the hit times, optionally with an amplitude weigth.

5.4 DipoleFit

DipoleFit (DF) is also a very simple method, it calculates the unit vector from one OM to the next hit OM as an individual dipole moment. The average over all these dipole moments give the global moment M. It is calculated in two steps. First, all hits are sorted according to their hit times and then the dipole moment M is calculated.

You can find further information about the reconstruction procedures in [5].

6 Software and Simulation with MonteCarlo

For my complete analysis I used the *ICEREC*-software out of the release V01-05-02.
It is important to identify and discriminate signals in the detector which are caused by different particles. Therefore such particles are simulated. The AMANDA simulations are done in a chain of subsequent steps with different software packages. These packages are managed by a series of Perl scripts called *Simuperl*. The specific output of AMANDA simulation is a (.F2k) plain-text format.

6.1 dCorsica

dCorsica is a cosmic ray generator specifically adapted for AMANDA and IceCube. The simulation package is based on the software package **CO**smic **R**ay **SI**mulations for **CA**scade experiment (CORSICA). It simulates atmospheric muons from highly energetic cosmic ray particles which interact with the earth atmosphere. This produces the already discussed down-going-muons. Simulations and the other software packages are based on former physical results and simulate the real life very well.

6.2 Nusim

Nusim is a neutrino generator. It generates a flux of atmospheric muons and signal muons which penetrate the earth. During their way neutral and charged interaction are simulated randomly. It is important to know, that the scattering angle between neutrino and lepton is always set to zero. Technically, you have to weight the simulated events for atmospheric and signal neutrino spectra.

7 Calculating of the geometrical track length in the detector

In the sketch in figure 7 you can roughly see how my algorithm works. I parameterize the AMANDA detector like a cylinder. The zero point is the middle of the detector. The radius, hight and depth of this cylinder is variable. To represent the AMANDA detector I have chosen the following parameters(see figur 8):

- Radius=92m
- Hight=240m
- Depth=-270m

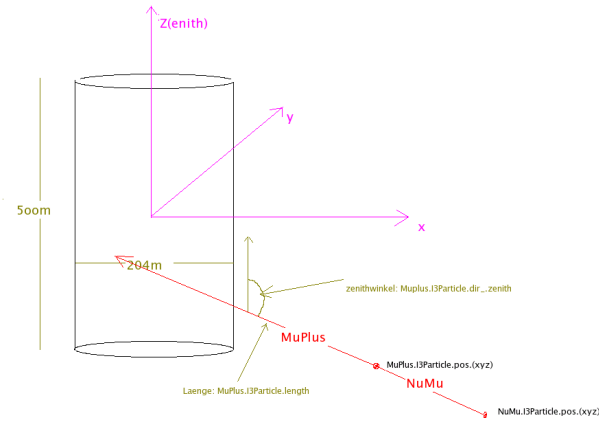

Figure 7: sketch of the "beer-can-model" for computing the geometrical track length in the detector

After I have checked if the muons start inside or outside the detector I computed the points of intersection of the muon track and an infinite high/depth cylinder. With the information about the start point of the muon and the direction (zenith and azimuth) a calculated a linear equation (in vector format) and computed the points of intersection with the cylinder formula $x^2 + y^2 = R^2$. Some events are already rejected in this step, because they do not hit the detector at all. In the next step I checked where these cuts are located, cylinder mantle, top, bottom or even no cuts in case of a location higher/lower the default hight/depth. Then I compare the complete track length with the points of intersection. There are three possibilities, the muon crosses the detector, the muon stops in the detector and the muon do not reach the detector. After all steps there is an output of all interesting parameters(see figure 10).

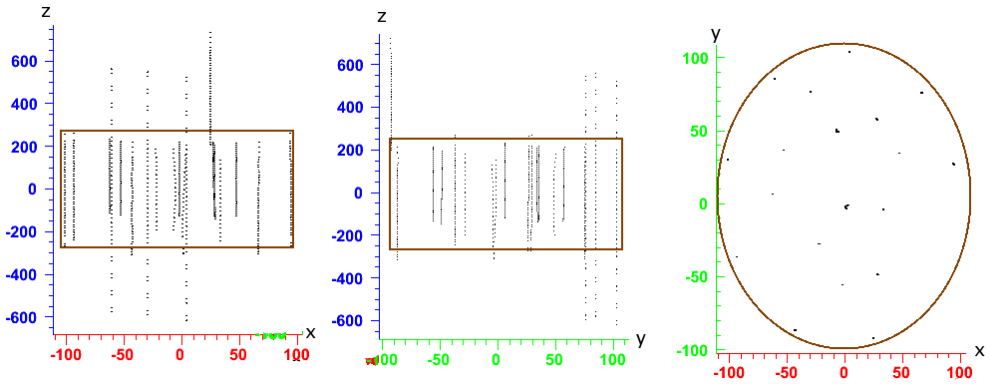

Figure 8: All AMANDA strings and OMs are visible and the chosen volume for computing the geometrical track length is marked.

In figure 9 you can see the the plots of the geometrical track length versus the zenith angle as well as a 3D-plot of all points of intersection. The expected shape is is visible. For a zenith angular of 0 or π rad we calculated the complete hight of the cylinder(510m) and for zenith angular of about $\pi/2$ we get twice the radius(184m).

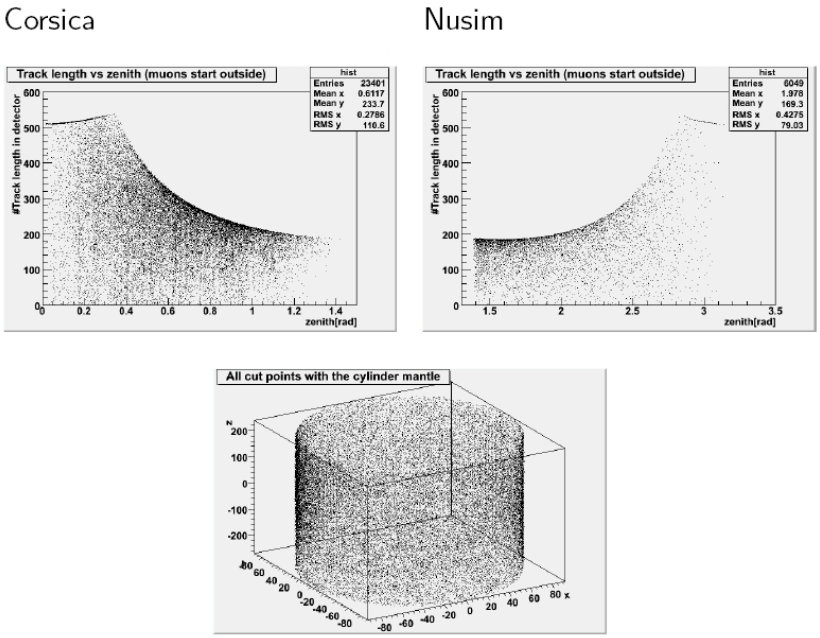

Figure 9: Top: geometrical track length versus the zenith angle for nusim and dcorsica files; bottom: 3D-plot of all points of intersection which forms the expected cylinder

If you compare the x- and y-distribution of the muons (nusim: -10000m up to 10000m, dcorsica:-5000 up to 5000) with the z-distribution (nusim: up to -1300m, dcorsica: up to 1700m) it is perfectly clear that the most muons cross the detector with an internal length of twice of the radius. For nusim this peak is more steepen because of the bigger x-y-range for the muon start points (figure 10).

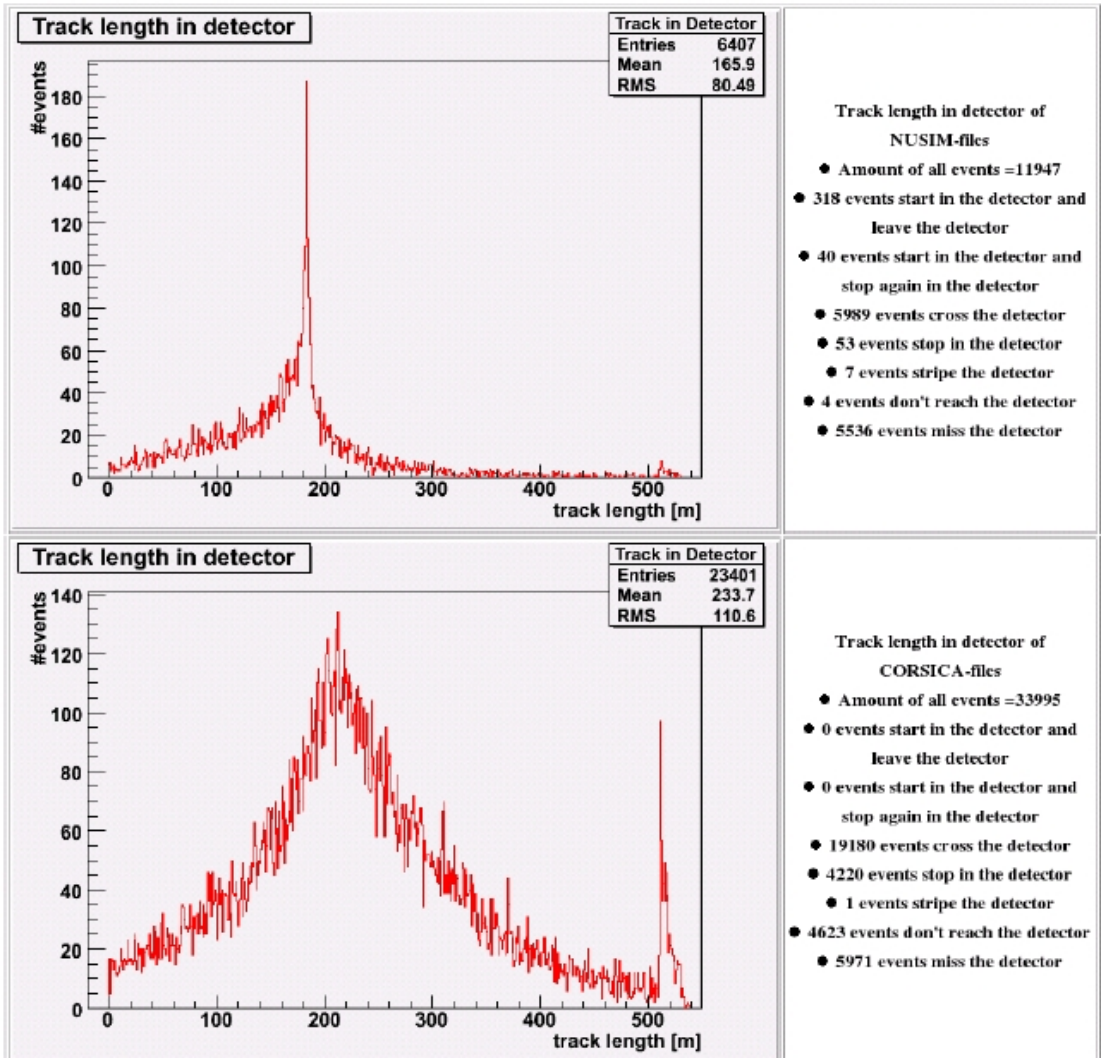

Figure 10: Some results for nusim (top) and corsica (bottom) files, with the appendant output.

8 Verification of AMANDA-dCorsica data

8.1 General remark

The MC input files for this study are standard F2K-AMASIM-dcorsica files (2003 detector configuration). After creating pulses there is a hit cleaning which suppresses noise. For AMANDA we used a hit cleaning called *I3Isolated HitsCutModule*. This pulse selection module rejects all pulses which are temporally and/or spatially isolated. We adjust the parameters so that the module count pulses within a radius of 50m and a time range of 1000ns. All pulses that have a smaller count than multiplicity=1 are rejected. We also rejected some OMs (full string 17 and the OMs of string 11, 12 and 13 which are only used to study ice-properties). Then the reconstructed pulses were used for DirectWalk, LineFit and DipoleFit provided they have enough hits. We adjusted a under limit for reconstruction. Only events with ≥ 24 hits are reconstructed. All others are tagged.
You can get more information from the Python-script in appendix.

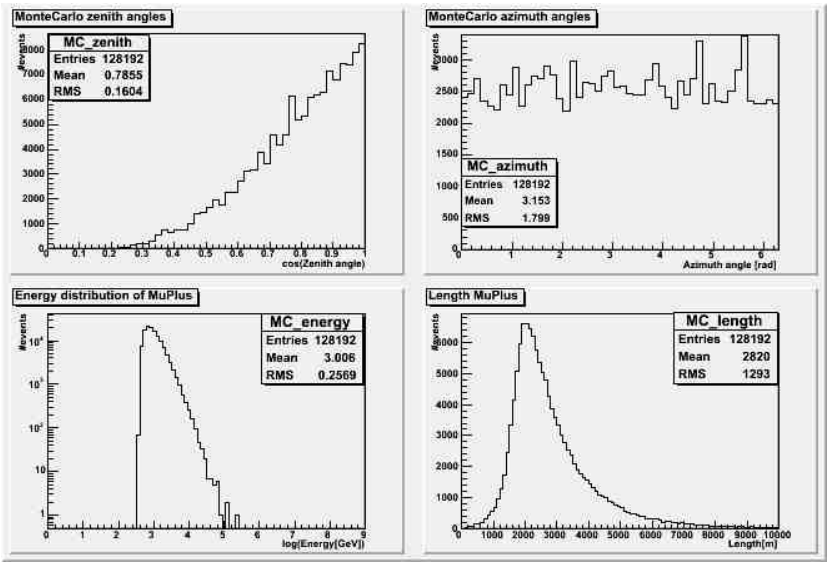

Figure 11: Histograms about *top left*:zenith distribution, *top right*:azimuth distribution, *bottom left*:energy distribution, *bottom right*:muon full track length distribution for atmospheric muons.

8.2 Properties of the true track

The most important information is the angular distribution of zenith and azimuth of the simulated true tracks. In figure 11 (top) you can see both distributions. It is clear that the azimuth is flat between 0 up to 2π. As dcorsica

simulates down-going atmospheric muons, the zenith range is limited from 0 up to $\pi/2$.

It is important to note that one dcorsica-event can contain several muons with nearly similar angles of incidence on the ice surface. For the full amount of events which can be reconstructed the number of all muons (μ^+ and μ^-) is 2.5 times higher. In case of an event with more muons, the first guess method finds (or finds not) a solution for the hits from all muons and cannot discriminate between these muons. Therefore such events have a bigger weighting than events with only one muon. But it is to note, that these effects are not essentially.
In figure 11 (bottom left) you can also see the energy distribution of the muons. The muon energy distribution peaks at about $log(E = 500GeV) \approx 2.7$. This is minimal necessary energy for a muon to reach the detector deep in the ice. You can also see an descent up to the fewest muons with energies of about $log(E[GeV]) \approx 5.3$. In the last histogram in figure 11 (bottom right) you see the complete muon track length from the starting point in the ice up to location where the muon stops.
Information about the strings and OMs plus the number of hits per event you can get in figure 12. You have to remember that these plots were produced after hit cleaning. Without hit cleaning there is a strong peak at 18 in the string distribution. These plots are interesting to compare with the plots for the signal muons in the next chapter.

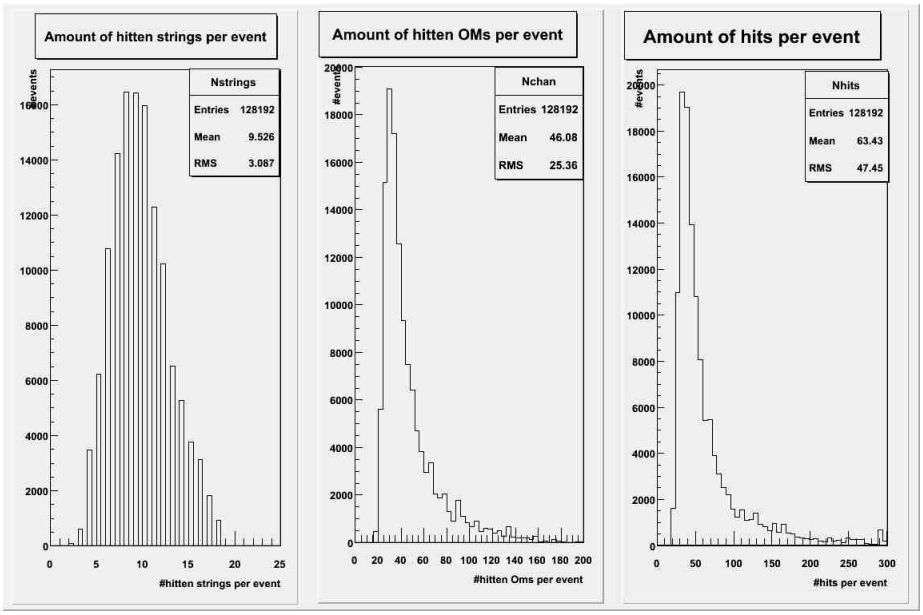

Figure 12: Histograms of the amount of strings (left) and OMs (middle) on target plus the amount of hits per event

8.3 Properties of the reconstructed tracks

In this chapter I want to describe the reconstructions of DirectWalk, LineFit and Dipolefit and compare their results. In Figure 13 you can compare the several reconstruction procedures with the MC-true-track. Because of the different reconstruction procedures, the number of reconstructed events differs. So you have only to compare the shape of the graphs. You can see that all first guess method nearly reconstruct all MC events. For azimuth and zenith LF and DF looks very similar. Important to note is that for all procedures some events are reconstructed in the wrong direction(see middle panel in figure 13).

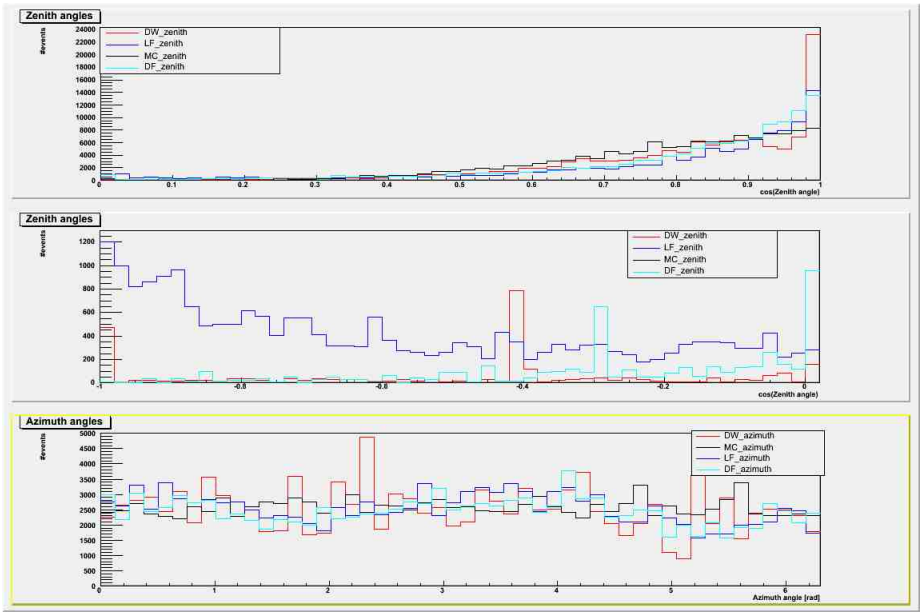

Figure 13: Plots of the MC-true-angles and the reconstructed angles with DirectWalk, LineFit and DipoleFit.

Information about the DW reconstruction parameters are plotted in figure 14. In the top left panel you see distribution of hits which were available for the reconstruction with a mean value about 67 hits per event. However you see in the top right panel the amount of hits which were used for reconstruction (mean ≈ 28). In the middle panels you see in the left panel the length distribution (calculated with DW) and in the right the average distance to the DW-track-element. These parameters depend on the requirement in the $\delta t - \rho - plane$ (see [10][11]). Plots about the amount of direct hits and calculated track length (with I3CutsModule) are visible in the lower panel. The most reconstructed events have about five direct hits and a length about 190m. The track length distribution in the lower left panel has a peak at zero which is unusual and not explicable yet.

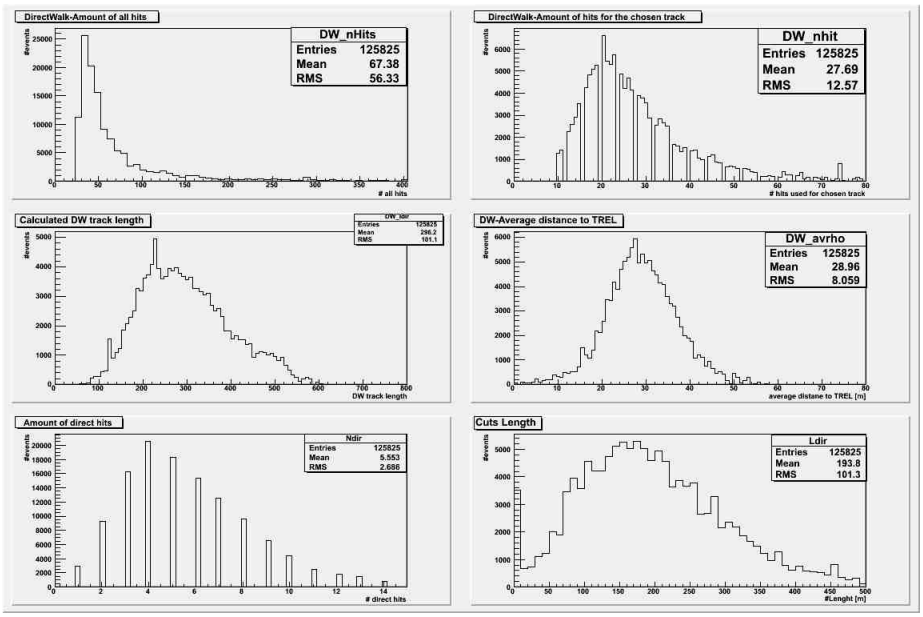

Figure 14: Reconstruction parameters of DirectWalk

8.4 Accuracy and Resolution

In this chapter I compare the several reconstruction procedures in detail. After calculating the differences between the MC-true-track and the reconstructed zenith and azimuth angle I fitted a gauss shape into the Δzenith peak to determine the resolution out of the sigma (See figure 15 and 16). The results are offered in the following table. The best result, which we can expect, is a single peak at zero with a small sigma. The small tail in negative direction in the Δzenith LineFit plot is coming most likely from events which are reconstructed in the opposite direction (compare figure 99). In figure 99+6 there is also a graph of the angular deviation in space.

I also compute *fake-rates* and *efficiencies* for the several reconstruction procedures. The definitions of these parameters are:

- **Mis-recontruction:**Events which are reconstructed with an space-angle, that differs from the true one by $> 0.5rad$ (Definition by P.Steffen [**?**])
- **Efficiencies:**All reconstructed events divided by all events which have sufficient hits ($>$ minHits).
- **Fake-rate :**Events which are reconstructed in the opposite hemisphere.

First Guess Method	Zenith-Resolution [°]	Mis-reconstruction [%]	Efficiency [%]	Fake-rate [%]
DW	14	45	99	1.9
LF	18	63	100	16.7
DF	19	56	100	2.9

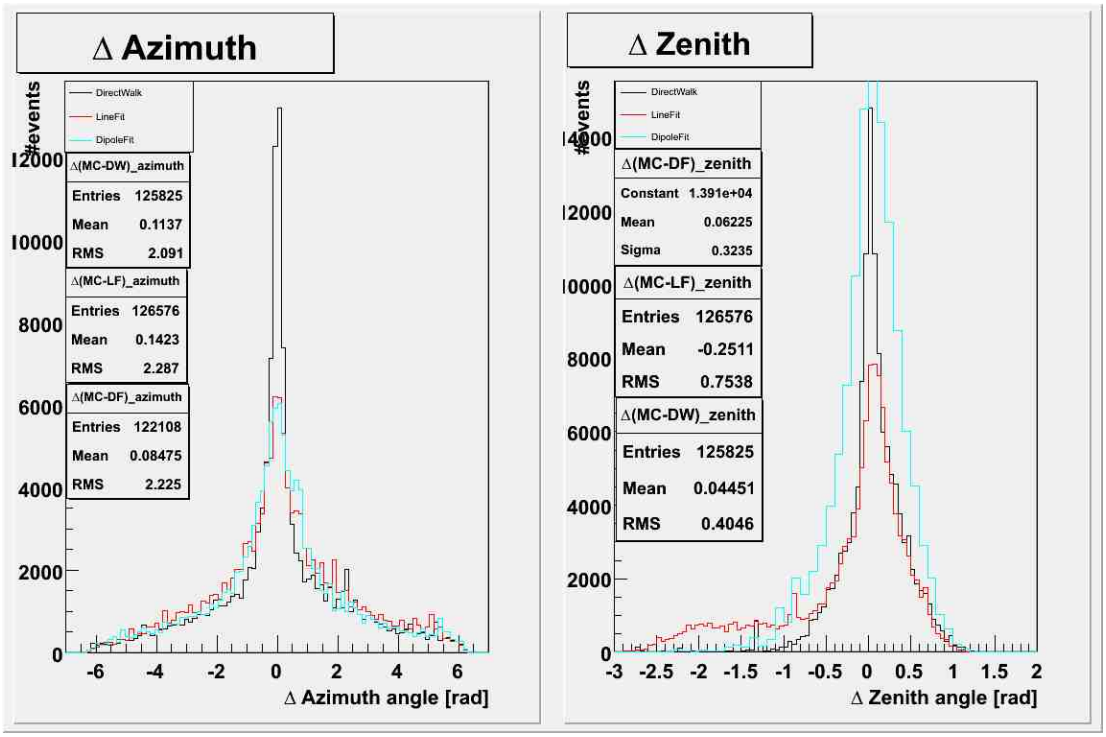

Figure 15: Distribution of $\Delta(MCtruetrack - reconstruction)$ for azimuth (left) and zenith (right) for all reconstruction procedures

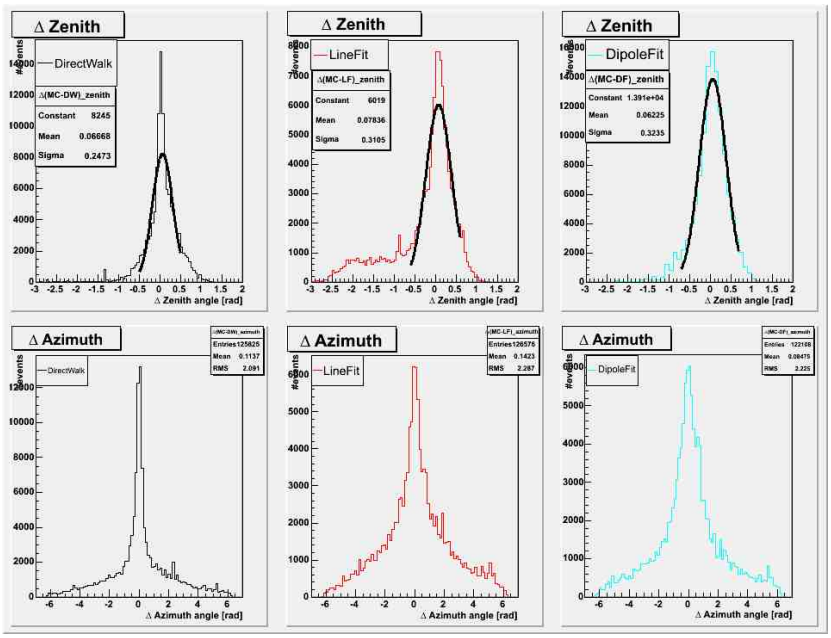

Figure 16: Distribution of $\Delta(MCtruetrack - reconstruction)$ for zenith (top) and azimuth (bottom)

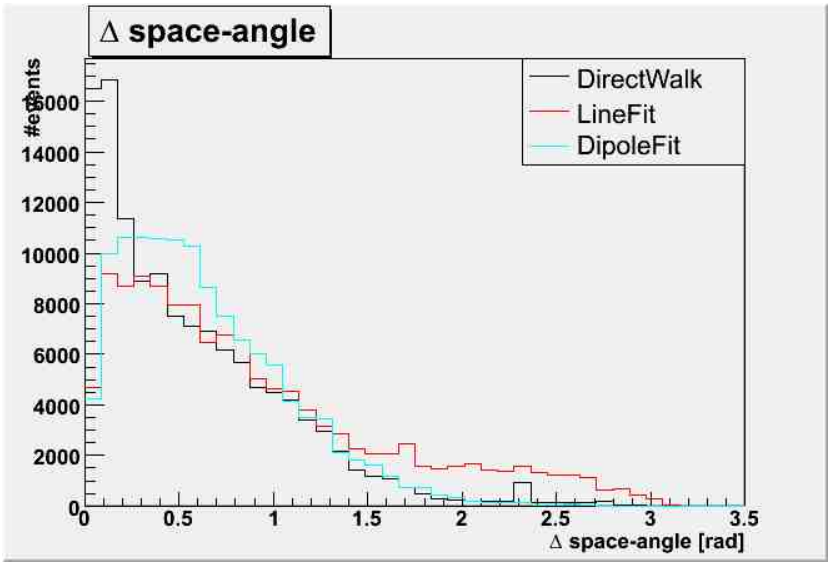

Figure 17: Space angle distribution of $\Delta(MCtruetrack - reconstruction)$ for AMANDA dcorsica

8.5 Dependence of the accuracy on the MC-true-zenith-angular

In this chapter I calculated the resolution of the first guess methods in dependency on zenith angular ranges. I plotted the resolution against the mean value of bins in the zenith of the MC-true-track. On the Pole the events with an reconstructed zenith angle smaller then 70° will be not considered. Therefore it is necessary to have a good angular resolution for events with zenith angles bigger then 70°. These events could be some of the rare muons from signal neutrinos. One can see that the resolution worsens for tracks closer to the horizon for all reconstruction methods. This is less problematic for DW in magnitude and tendency (see figure 18). The mis-reconstructions (figure 19) are over a wide range constant. They only improve for zenith angles about zero.

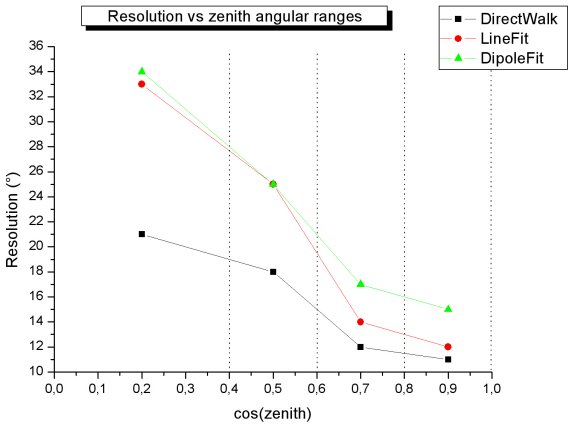

Figure 18: Dependence of the resolution on the MC-true-zenith-angular. The resolutions are plotted against the mean value of bins in the zenith of the MC-true-track.

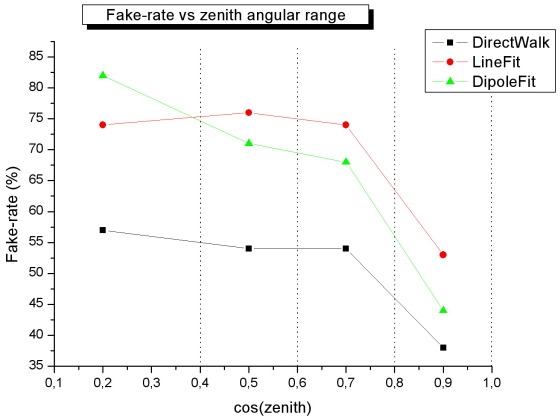

Figure 19: Dependence of mis-reconstructions on the MC-true-zenith-angular. The resolutions are plotted against the mean value of bins in the zenith of the MC-true-track

8.6 Dependence of the accuracy on the theoretical track length

We investigated if the geometrical length of the tracks in the detector volume is an indicator for a good reconstruction. Therefore, we compute the parameters for tracks which have a given minimal track length. In figure 20 you can observe the dependency of resolution and fake-rate on the geometrical track length. In case of longer theoretical tracks the resolution and fake-rate are smaller. In contrast the efficiency has no remarkable dependency on this length.

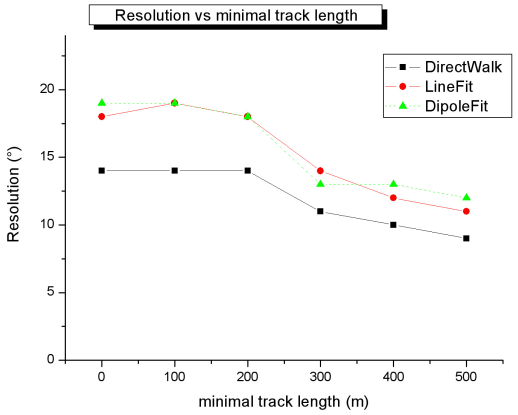

Figure 20: Dependence of the resolution on the geometrical track length in detector. The resolutions are plotted against the minimal chosen track length.

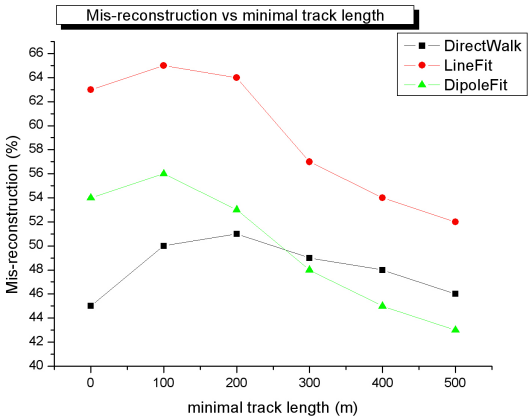

Figure 21: Dependence of the mis-reconstructions on the geometrical track length in detector. The resolutions are plotted against the minimal chosen track length.

8.7 Properties of unreconstructed events (only for DW)

If one uses DirectWalk for on-line filtering on the Pole it is important to know which properties belong to the unreconstructed, i.e. lost events. In figure 22 and 23 (full histograms) you can see the parameters of the 2% MC-true-tracks which cannot be reconstructed. It is evident, that these events have low energy and a short track length. It is also clear for figure 23 that these events have fewer hits on fewer strings and OMs. It is to note, that the distributions in figure 22 follow the distribution of the full sample.

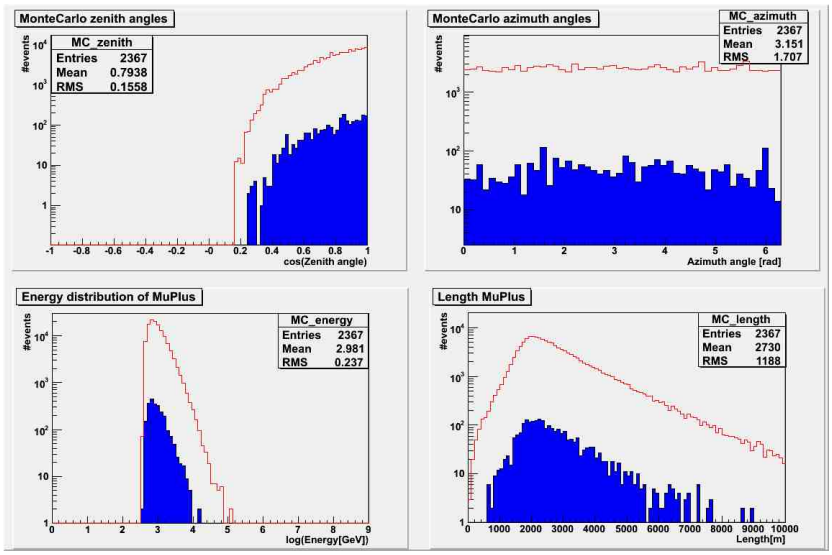

Figure 22: Histograms of MC-true-tracks which cannot be reconstructed by DirectWalk (full histogram) compared to the whole number of events (red curve). *top left*: zenith distribution, *top right*: azimuth distribution, *bottom left*: energy distribution, *bottom right*: muon full track length distribution for atmospheric muons.

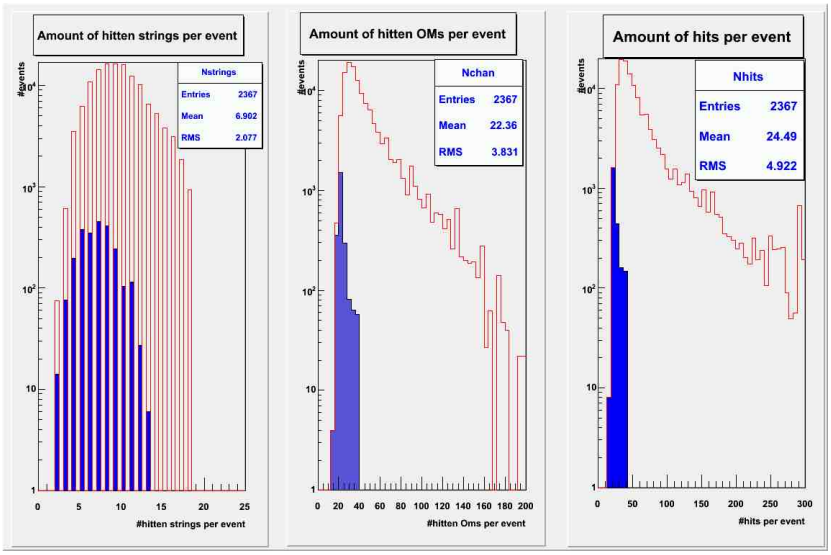

Figure 23: Histograms of the amount of strings (left) and OMs (middle) on target plus the amount of hits per event for events which cannot be reconstructed by DirectWalk (full histogram) compared to the whole number of events (red curve)

9 Verification of IceCube-dCorsica data (minHits>8)

9.1 General remark

The MC input files for this study are 9string F2K-AMASIM-dcorsica files (2006 detector configuration). For IceCube we used a hit cleaning called *I3Coincify*. This module is used to apply a Local Coincidence window to RecoPulseSeries. The number of nearest neighbors was adjusted to two and the time window for local incidence to 1000ns. All other pulses which do not fulfil these condition are rejected. Then the reconstructed pulses were used for DirectWalk, LineFit and DipoleFit provided they have enough hits. For IceCube only events with more than 8 hits are reconstructed. All events with less hits are tagged.

9.2 Properties of the true track

The properties of the true track are similar to the MC-true-track of the AMANDA-dcorsica files (compare figure 24 and 11). We have again a lot of events that contain several muons with nearly similar angles of incidence. The full amount of events which can be reconstructed is 49997, but the number of all muons (μ^+ and μ^-) is 95575. Information about the strings and OMs on target plus amount of hit per event you can get in figure 25. Because of bigger distances between the several strings and OMs the number of strings and OMs on target

and the hits per event are much smaller then for AMANDA geometry. The mean value for strings on target is about 2, for OMs on target it is 13 and for hits per event it is 14. But you have to remember that we only have 9 strings for IceCube in 2006.

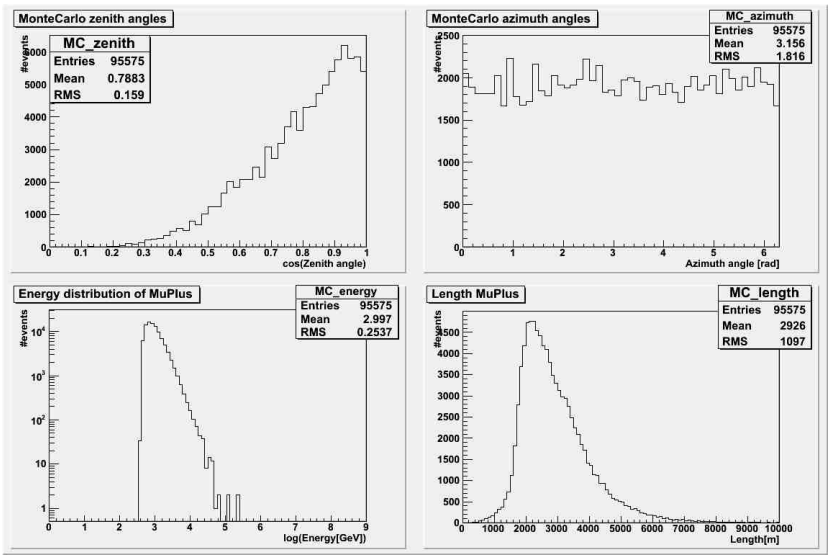

Figure 24: Histograms about *top left*:zenith distribution, *top right*:azimuth distribution, *bottom left*:energy distribution, *bottom right*:muon full track length distribution for atmospheric muons.

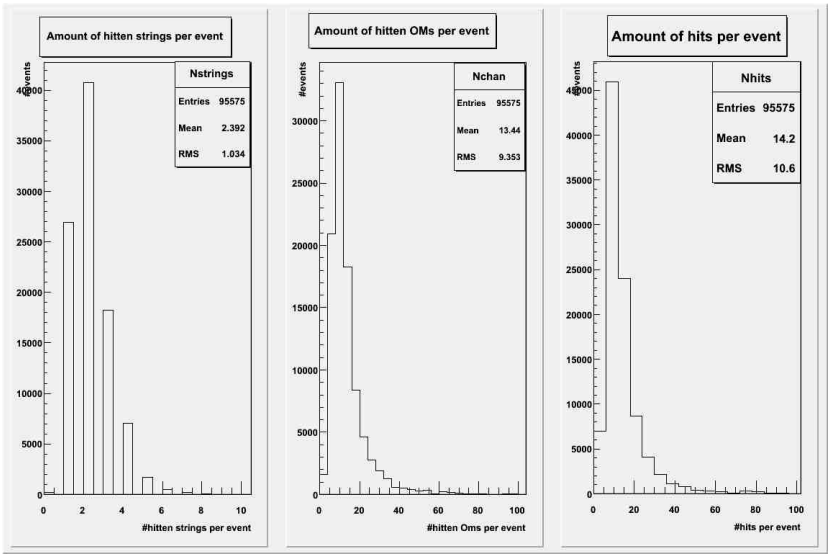

Figure 25: Histograms of the amount of strings (left) and OMs (middle) on target plus the amount of hits per event

9.3 Properties of the reconstructed track

In Figure 26 you can compare the several reconstruction procedures with the MC-true-track. Its important to know, that about 20% for all events (muons) could not be reconstructed because they had insufficient hits (< 8). LineFit and DipoleFit nearly reconstruct all MC events compared to DirectWalk which only reconstruct about 25%. For azimuth and zenith LF and DF looks very similar. For azimuth both curves have some notable high peaks on same places. However DirectWalk has only a notable peak for zero degree azimuth angles. These behaviors require further analysis.

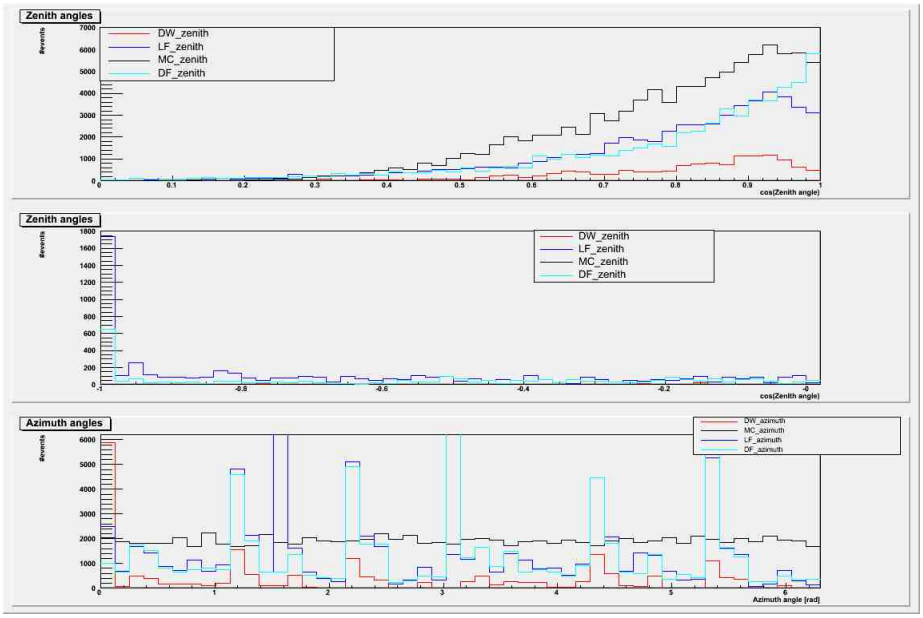

Figure 26: Plots of the MC-true-angles and the reconstructed angles with DirectWalk, LineFit and DipoleFit.

Information about the DW reconstruction parameters are plotted in figure 27. In the top left panel you see distribution of hits which were available for the reconstruction with a mean value about 29 hits per event. However you see in the top right panel the amount of hits which were used for reconstruction (mean ≈ 15). One can see that the mean value of all hits per event is much smaller as for AMANDA (mean ≈ 67) but the number of hits used for reconstruction is nearly the same. Because of IceCube geometry the calculated track length are longer then in AMANDA and the number of direct hits is smaller.

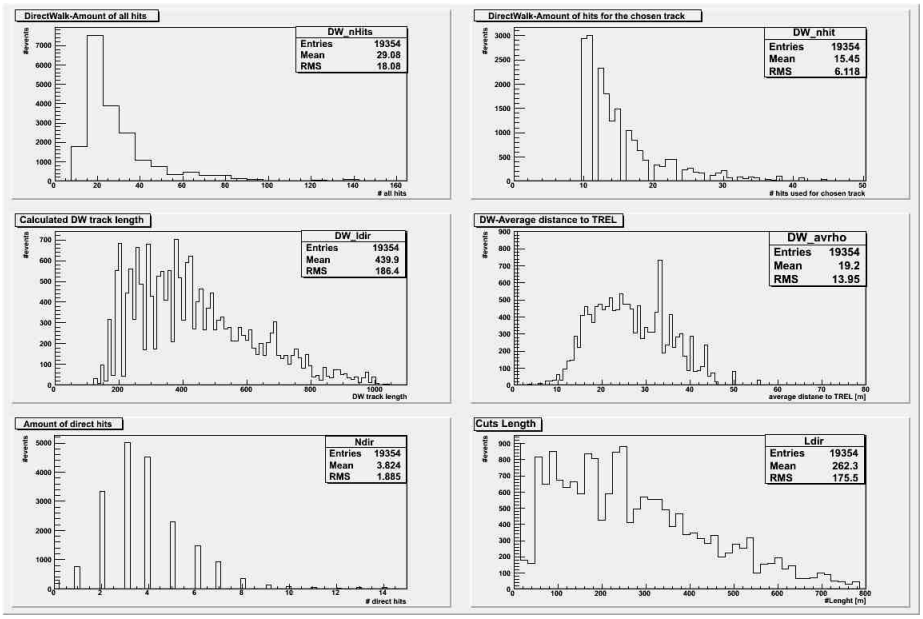

Figure 27: Reconstruction parameters of DirectWalk

9.4 Accuracy and Resolution

The resolutions, mis-reconstructions, efficiencies and fake-rates are calculated like in section 8.4. The delta peaks in figure 28 and 29 and the space angle distribution of $\Delta(MCtruetrack - reconstruction)$ show no unusual signs. The results are offered in the following table. One can see again, that the reconstruction of DirectWalk is the best also for the IceCube geometry. The DW-resolution and the fake-rate is even better then for AMANDA. But the efficiency is much smaller because of fewer hits in the IceCube detector.

First Guess Method	Zenith-Resolution [°]	Mis-reconstructions [%]	Efficiency [%]	Fake-rate [%]
DW	8	34	26	0.2
LF	16	47	100	7.2
DF	17	45	100	3.4

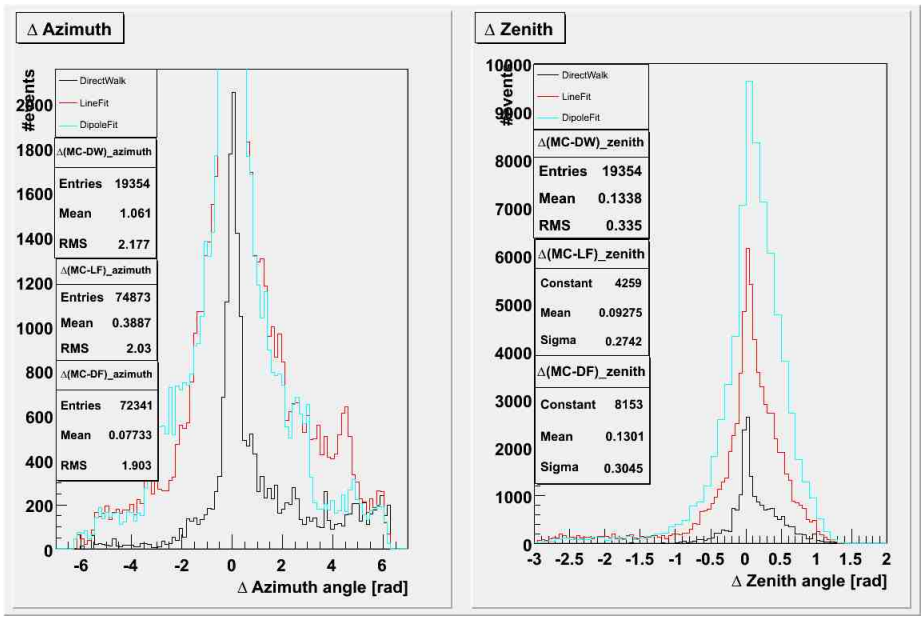

Figure 28: Distribution of $\Delta(MCtruetrack - reconstruction)$ for azimuth (left) and zenith (right) for all reconstruction procedures

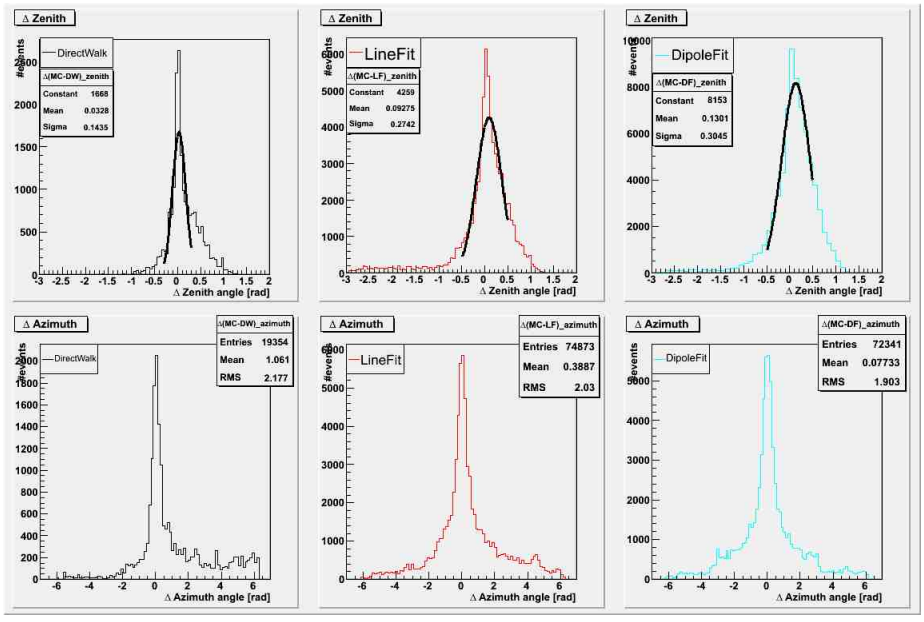

Figure 29: Distribution of $\Delta(MCtruetrack - reconstruction)$ for zenith (top) and azimuth (bottom)

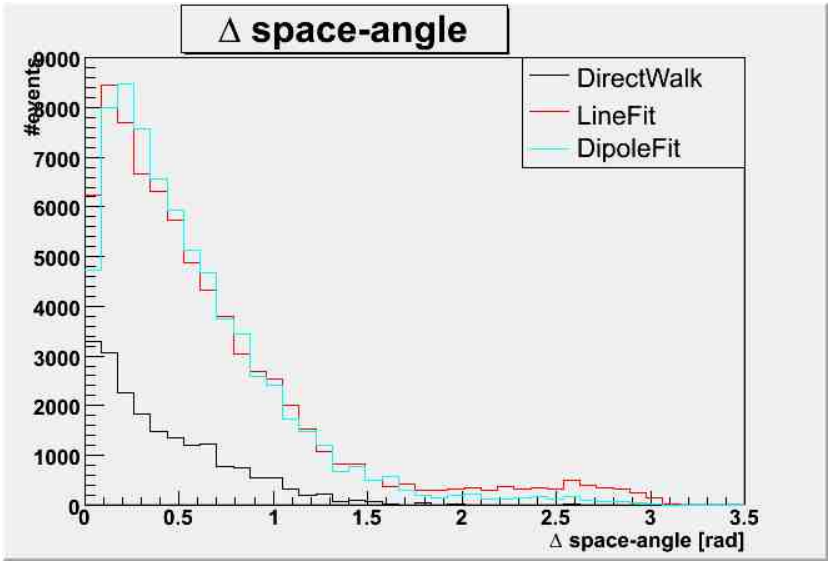

Figure 30: Space angle distribution of $\Delta(MCtruetrack - reconstruction)$ for IceCube dcorsica

9.5 Dependence of the accuracy on the MC-true-zenith-angular

Like in chapter 8.5 I plotted the resolution, the mis-reconstruction-rate and the fake rate against the mean value of bins in the zenith of the MC-true-track (see figures 31,32,33). The behavior is similar to AMANDA. For the resolution plot there are only small deviations. But the resolution becomes also smaller for all reconstruction methods. The LineFit and DipoleFit mis-reconstruction-rate and fake-rate have big dependency on the bins in the zenith. These values worsens for tracks closer to the horizon. In the case of DirectWalk only the mis-reconstruction-rate decreases. The fake-rate is nearly constant zero.

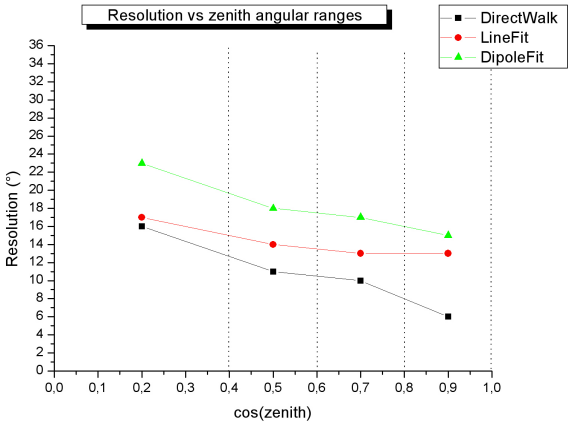

Figure 31: Dependence of the resolution on the MC-true-zenith-angular. The resolutions are plotted against the mean value of bins in the zenith of the MC-true-track.

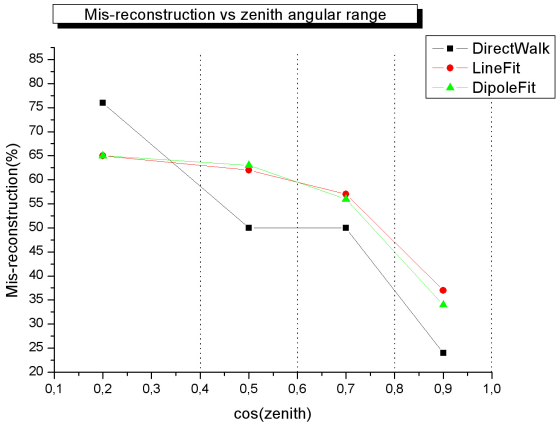

Figure 32: Dependence of the mis-reconstruction-rate on the MC-true-zenith-angular. The resolutions are plotted against the mean value of bins in the zenith of the MC-true-track.

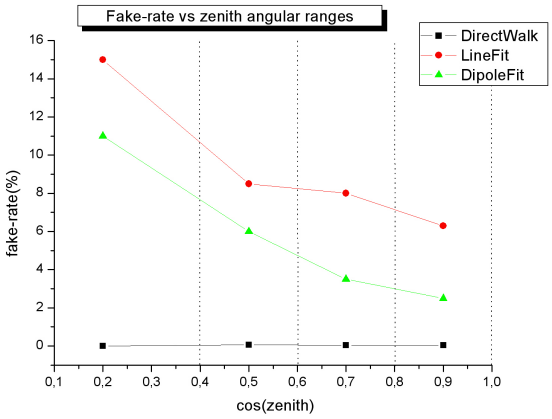

Figure 33: Dependence of the fake rate on the MC-true-zenith-angular. The resolutions are plotted against the mean value of bins in the zenith of the MC-true-track.

9.6 Properties of unreconstructed events (only for DW)

In figure 34 (full histogram) you can see the parameters of the MC-true-tracks which cannot be reconstructed. The efficiency of the DW reconstruction is about 25%. One can see, that there is no evidence for special ranges for the parameters in figure 34. In contrary the number of hits and OMs on target is comparable small for events which are not reconstructed (see figure 35).

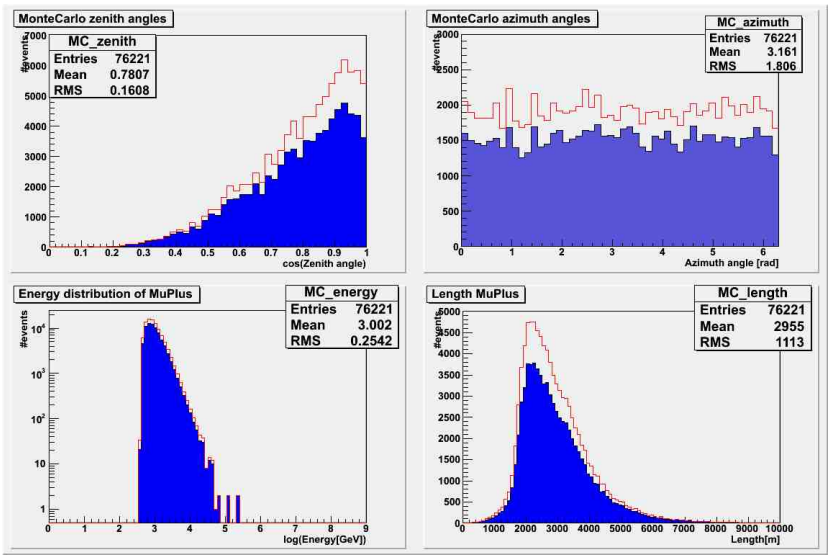

Figure 34: Histograms of MC-true-tracks which cannot be reconstructed by DirectWalk (full histogram) compared to the whole number of events (red curve). *top left*: zenith distribution, *top right*: azimuth distribution, *bottom left*: energy distribution, *bottom right*: muon full track length distribution for atmospheric muons.

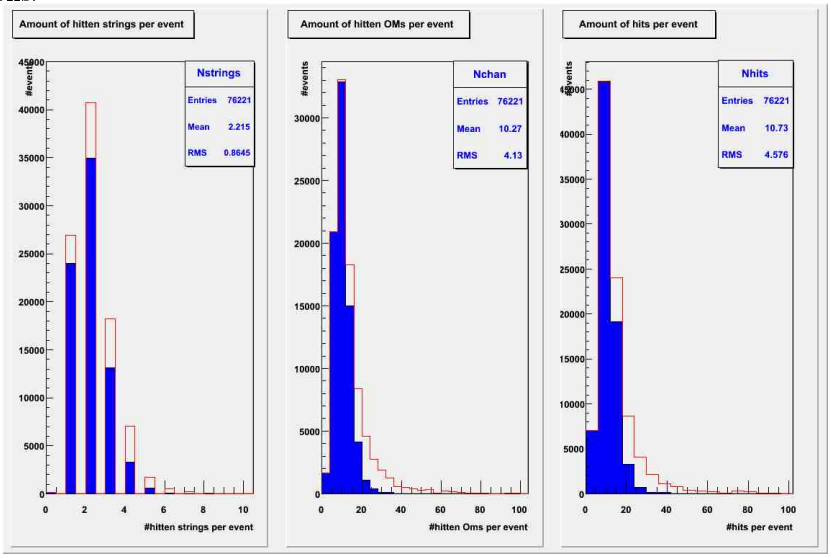

Figure 35: Histograms of the amount of strings (left) and OMs (middle) on target plus the amount of hits per event for events which cannot be reconstructed by DirectWalk (full histogram) compared to the whole number of events (red curve)

10 Verification of IceCube-dCorsica data (minHits>16)

10.1 General remark

The only difference to the previous chapter is, that there are only events with more then 16 hits. In this case it is clear that the whole number of events becomes smaller (only 25% of the whole amount in the previous chapter).

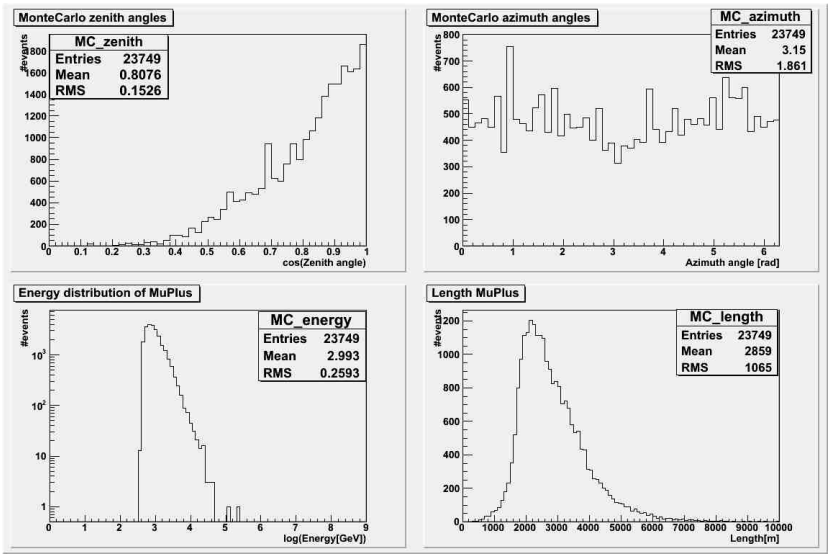

Figure 36: Histograms about *top left*:zenith distribution, *top right*:azimuth distribution, *bottom left*:energy distribution, *bottom right*:muon full track length distribution for atmospheric muons.

10.2 Properties of the true track

The properties of the true track are nearly the same as the MC-true-track of the sample in the previous chapter (compare figure 36 and 24). Information about the strings and OMs on target plus amount of hit per event you can get in figure 37.

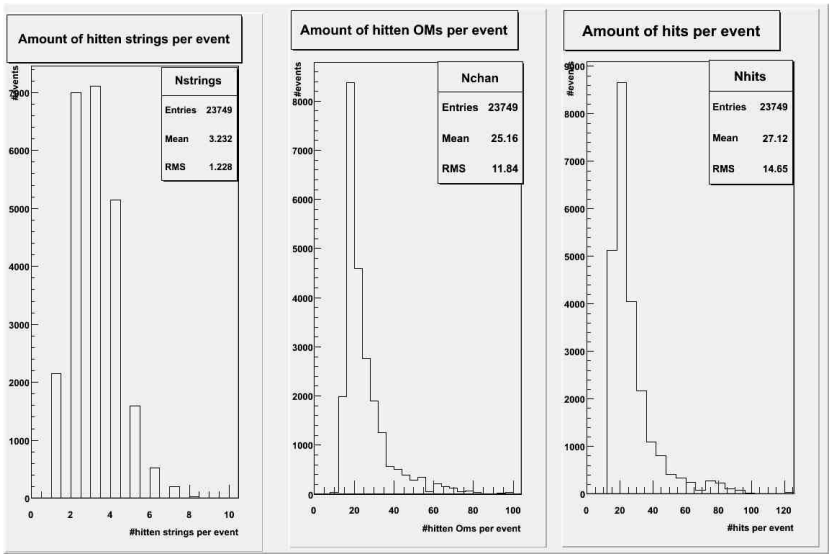

Figure 37: Histograms of the amount of strings (left) and OMs (middle) on target plus the amount of hits per event

10.3 Properties of the reconstructed track

In Figure 38 you can compare the several reconstruction procedures with the MC-true-track. LineFit and DipoleFit reconstruct nearly all MC-true-tracks and DirectWalk about 70%. One can see that the DirectWalk algorithm needs more then 16 hits for a reconstruction with good efficiency.

Information about the DW reconstruction parameters are plotted in figure 39. These values are nearly identical to the values in figure 27 out of the previous chapter.

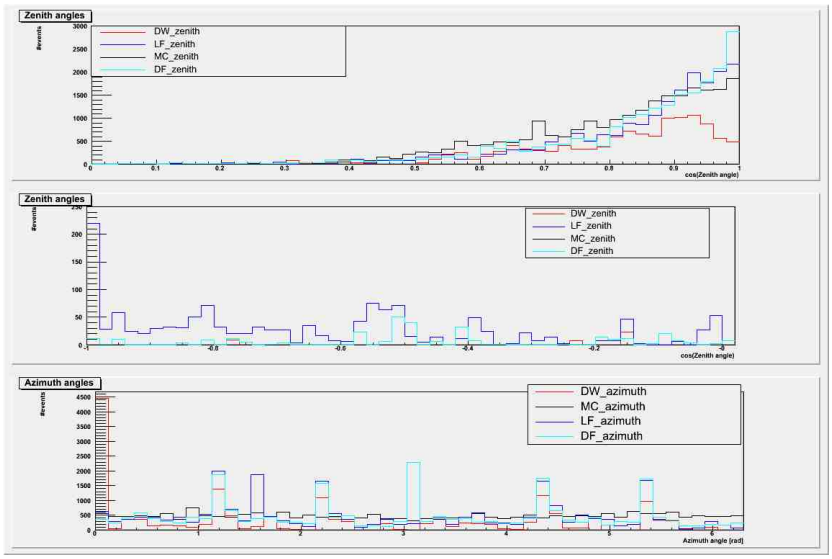

Figure 38: Plots of the MC-true-angles and the reconstructed angles with DirectWalk, LineFit and DipoleFit.

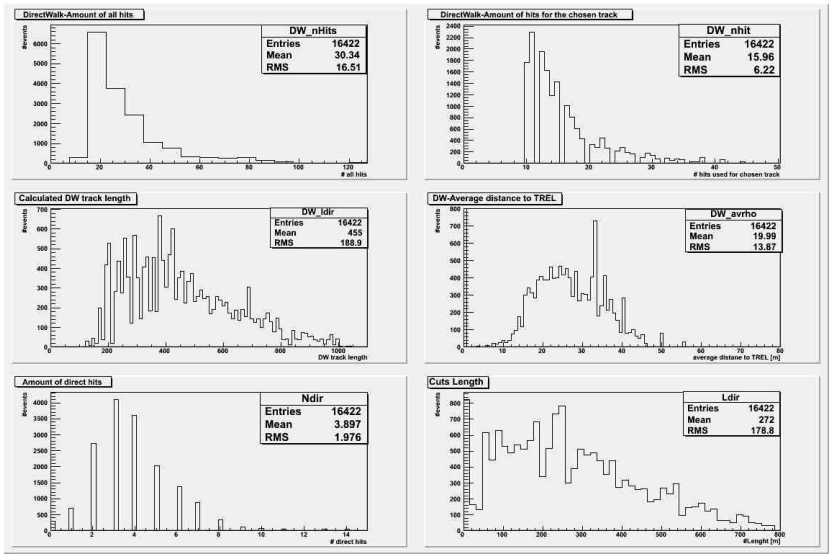

Figure 39: Reconstruction parameters of DirectWalk

10.4 Accuracy and Resolution

The parameters for the accuracy analysis are calculated like in the previous chapters and are located in the following table. The delta plots are visible in figure 40 and 41 and the space angle plot in figure 42. It is obviously that the accuracy becomes better for a reconstruction with more hits. The samples which are used in this chapter and in the previous chapter are the same. The only difference is, that we have rejected the events with a number of hits fewer than 16. After this re-triggering the accuracy for all reconstruction methods is better.

First Guess Method	Zenith-Resolution [°]	Mis-reconstructions [%]	Efficiency [%]	Fake-rate [%]
DW	8	31	69	0.25
LF	12	35	100	5.8
DF	13	32	100	1.25

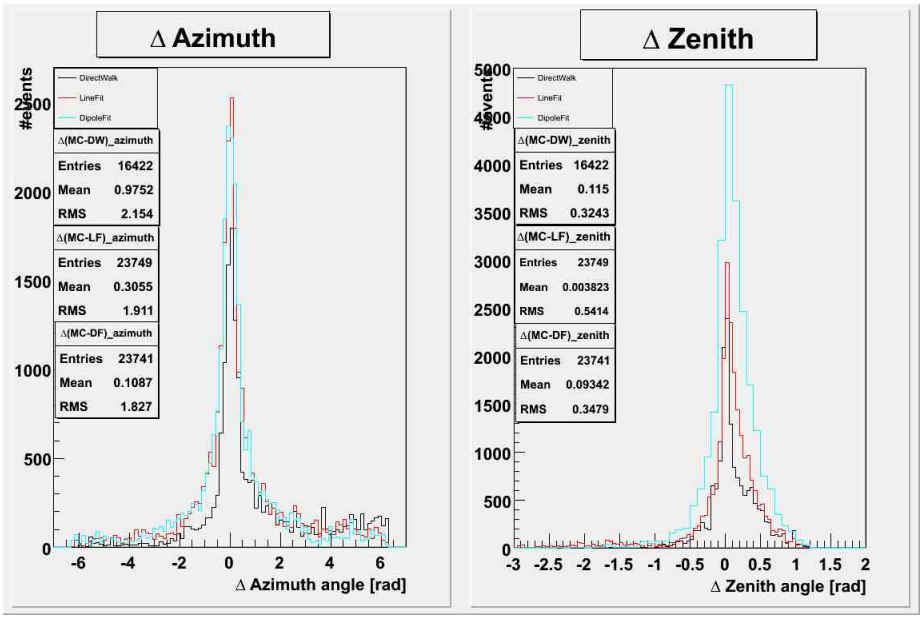

Figure 40: Distribution of $\Delta(MCtruetrack - reconstruction)$ for azimuth (left) and zenith (right) for all reconstruction procedures

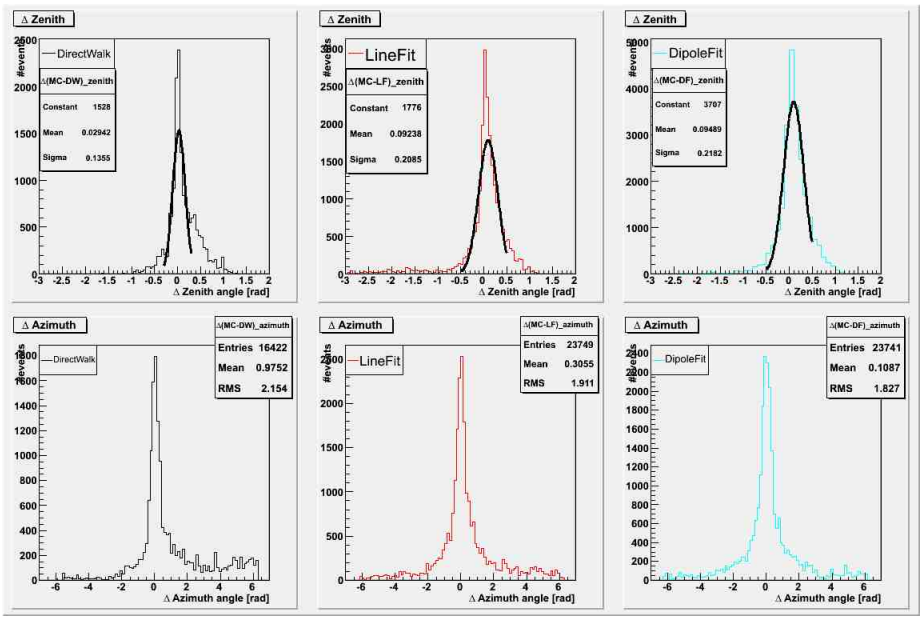

Figure 41: Distribution of $\Delta(MCtruetrack - reconstruction)$ for zenith (top) and azimuth (bottom)

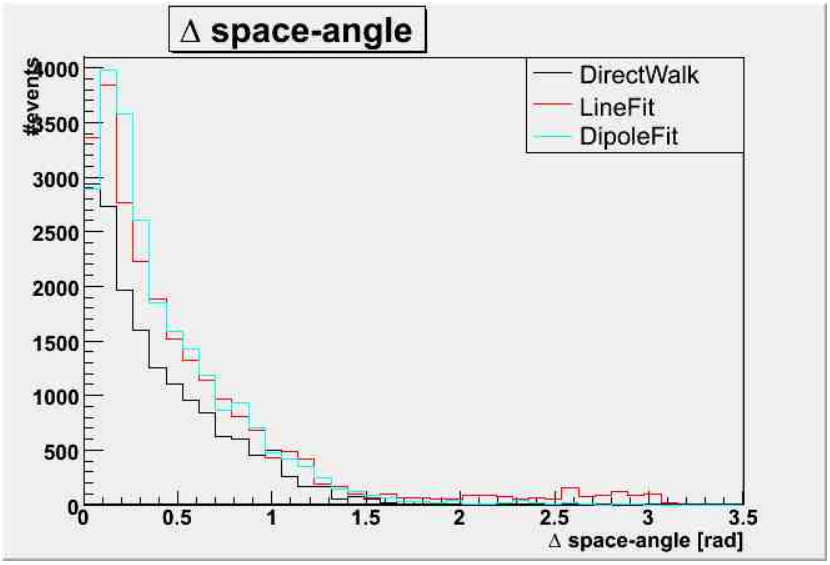

Figure 42: Space angle distribution of $\Delta(MCtruetrack - reconstruction)$ for IceCube dcorsica- events (minHits>16)

10.5 Dependence of the accuracy on the MC-true-zenith-angular

The plots of resoulution, mis-reconstruction-rate and fake-rate versus the mean value of bins in the zenith of the MC-true-track are visible in figure 43,44 and 45. The behavior is nearly the same as in section 9.5.

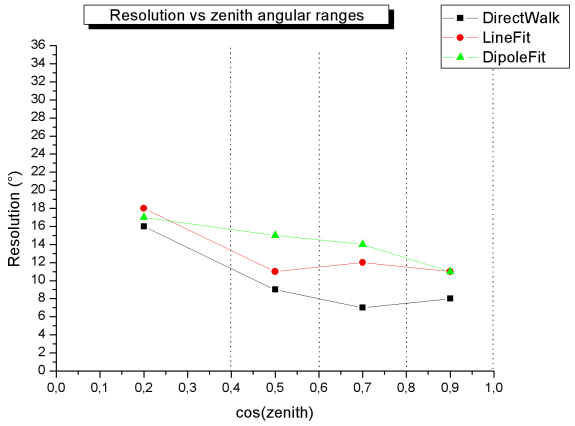

Figure 43: Dependence of the resolution on the MC-true-zenith-angular. The resolutions are plotted against the mean value of bins in the zenith of the MC-true-track.

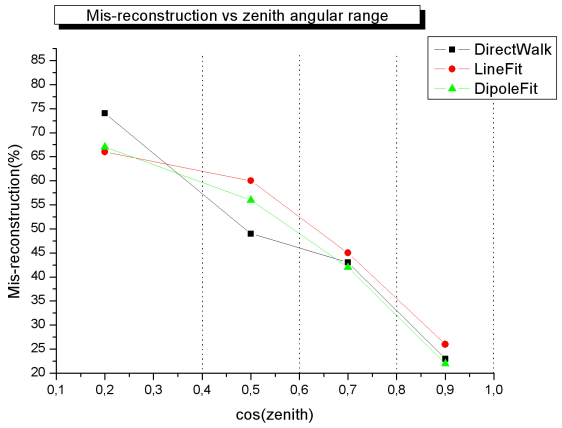

Figure 44: Dependence of the mis-reconstruction-rate on the MC-true-zenith-angular. The resolutions are plotted against the mean value of bins in the zenith of the MC-true-track

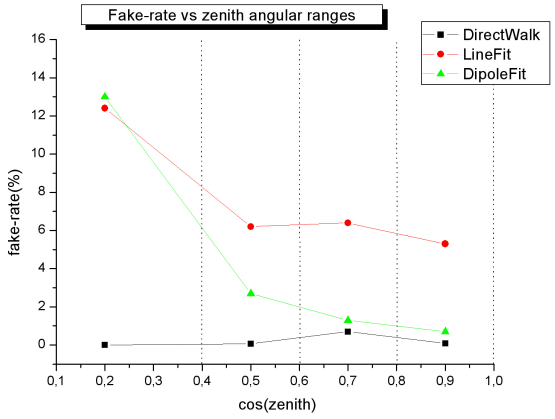

Figure 45: Dependence of the fake rate on the MC-true-zenith-angular. The resolutions are plotted against the mean value of bins in the zenith of the MC-true-track

10.6 Properties of unreconstructed events (only for DW)

In figure 46 and 47 (full histograms) one can see the parameters of the MC-true-tracks which cannot be reconstructed. The knowledge is the same as in previous chapter. The only difference is, that more events were reconstructed.

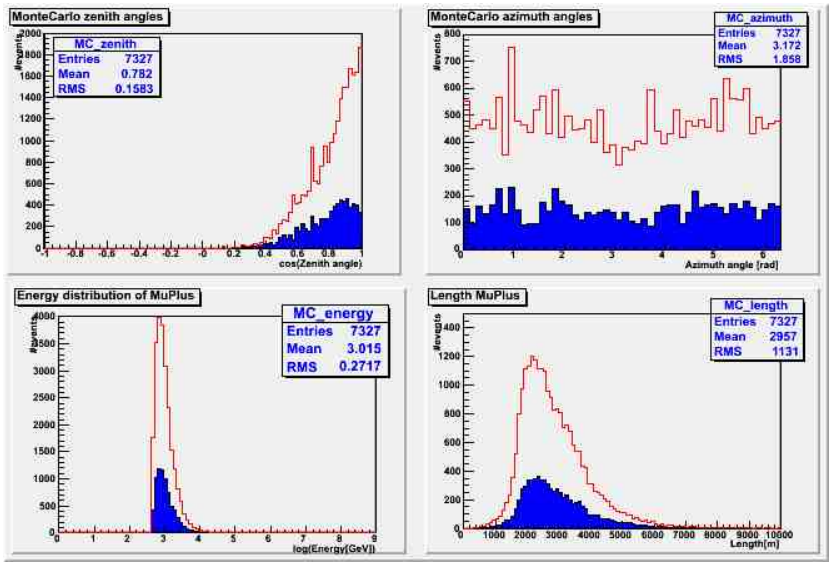

Figure 46: Histograms of MC-true-tracks which cannot be reconstructed by DirectWalk (blue curves) compared to the whole number of events (red curve). *top left*:zenith distribution, *top right*:azimuth distribution, *bottom left*:energy distribution, *bottom right*:muon full track length distribution for atmospheric muons.

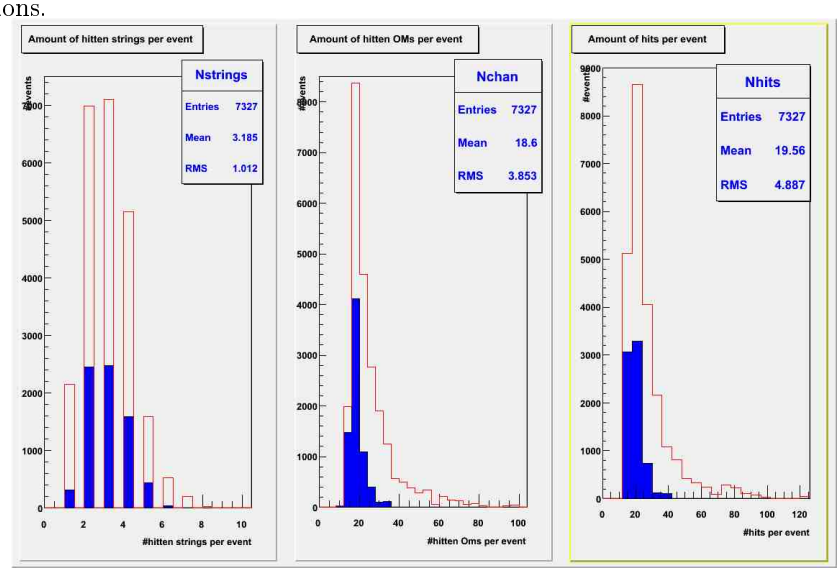

Figure 47: Histograms of MC-true-tracks which cannot be reconstructed by DirectWalk. *top left*:zenith distribution, *top right*:azimuth distribution, *bottom left*:energy distribution, *bottom right*:muon full track length distribution for atmospheric muons.

11 Conclusion

For the first time the DirectWalk algorithm, as implemented in IceRec, was used to analyse AMANDA and IceCube data - and compared to the LineFit and DipoleFit algorithms. The verification of DirectWalk in this study using dCorsica Monte Carlo event samples shows an consistent behavior as expected from previous studies. The number of the strings and OMs of the reconstructed events, the hits (and direct hits respectively) and the track lengths correspond to the specific geometries. The measurements of the reconstruction qualities demonstrated that DirectWalk is the superior reconstruction method for AMANDA (for the first guess methods under study), and also for a nine string IceCube set-up. DirectWalk has the best resolutions, fake-rates and the mis-reconstruction-rates for AMANDA and IceCube. A new method to verify DirectWalk was developed; it was based on the calculation of the geometrical track length. The verification for neutrino events needs further studies; they could lead to the usage of DirectWalk as method for on-line filtering

12 Acknowledgement

First I have to say, that it was a great time at DESY-Zeuthen. I have learned a lot of new things which are very important for research in astro particle physics. But what is research without nice and helpful colleagues? I will always remember this pleasant atmosphere in the AMANDA group. All persons were very friendly from the beginning until the end. Special thanks go to my supervisor Damian who divides his office with me and who was always willing to help me (and I had a lot of questions...). In addition special thanks to Stefan, a great group leader who supported me very often, Robert (my `Root`-specialist), Markus, Bernhard, Martin, Elisa and Mike. If I had forgotten someone, sorry, you all were great.

References

[1] Unsöld,A.; Baschek,B.: Der Neue Kosmos,Springer,Berlin,7.Aufl.

[2] DESY Zeuthen *Neutrino Astrophysics*, web site. URL http://www-zeuthen.desy.de/nuastro/

[3] T.Gaisser, *Outstanding Problems in particle Astrophysic*, e-print arXiv:astro-ph/0501195,2005.

[4] R.Lang, Diploma Thesis: *Search for Point Sources of High-Energy Neutrinos with the AMANDA Detector* (2005)

[5] Wiebusch et al. for the AMANDA Collaboration, *Muon Track Reconstruction and Data Selection in AMANDA*(2005)

[6] J.G.Learned, K.Mannheim, High-Energy Neutrino Astrophysics, Annual Reviews of Nuclear and Particle Science 50 (2000) 679-749

[7] The Barwick Group for the AMANDA collaboration, *AMANDA-II project-official site*, web site. URL http://amanda.uci.edu/.

[8] E.Andres et al. (the AMANDA collaboration), *The AMANDA neutrino telescope: principle of operation and first results*, Astroparticle Physics **13**(2000),1-20.

[9] E.Bernardini for the AMANDA collaboration, *New results from the AMANDA Neutrino Telescope*, Nuclear Physics B (Proceedings Supplements)**145**(2005),319-322

[10] P.Steffen,DESY Zeuthen,AMANDA Internal Report, *DirectWalk - A Fast Track Search Algorithm without Hit Cleaning*, (2001)

[11] P.Steffen,DESY Zeuthen,AMANDA Internal Report, *DirectWalk II - Improved Version of DorectWalk*, (2002)